

The development of the complex of pulse-modulation amplifiers of voltage and current

Abstract. In this paper the results of the development of a complex of pulse-modulation amplifiers of voltage and current, are presented. Parameters of the amplifier, such as range of output three-phase voltages and currents, show that the developed complex is not only not inferior to widely used amplifiers, but also surpasses them in terms of weight and dimensions. To demonstrate the adequate operation of the complex, the deviations of the gains, the accuracy and phase accuracy of the output voltage and current were determined, which do not exceed 5 % and 0.1° , respectively.

Streszczenie. W artykule opisano wzmacniacz prądu i napięcia wykorzystujący modulację impulsów. Otrzymany wzmacniacz jest nie gorszy od powszechnie używanych wzmacniaczy przy znacznie mniejszej wadze i wymiarach. Dokładność wzmocnienia wzmacniacza w przypadku napięcia wynosiła około 5% przy niedokładności fazy 0.1° . **Prosty wzmacniacz prądu i napięcia z modulacją impulsową**

Keywords: electric power system, amplifiers of current and voltage, development, tests.

Słowa kluczowe: wzmacniacz prądu i napięcia, modulacja impulsowa.

Introduction

The reliable operation of relay protection and automation system (RPA), and electric power system (EPS) in a whole, is mainly determined by the correctness of their functioning algorithms, correspondence of the choosing parameters and calculated settings to the actual operation conditions of the RPA and EPS.

Nowadays modern RPA are complex, highly organized devices with wide logical and mathematical functionality. So, tasks of adequate setting up and testing of such devices become even more complex and require the availability of the necessary equipment: a simulation system (hardware real-time simulation system, and signal amplifiers for closed loop testing/hardware-in-the-loop (HIL) simulation of the real RPA [1, 2, 3]. This test method allows the most complete investigation of the main features of RZA.

The scheme of HIL simulation includes a signal source (for example, simulation system like a RTDS [4, 5], HYPERSIM [6], Hybrid Real-Time Power System Simulator (HRTSim) [7, 8]), wherein the part of EPS and the protected object are modeled), amplifiers of voltage and current, and a tested RPA (Fig. 1).

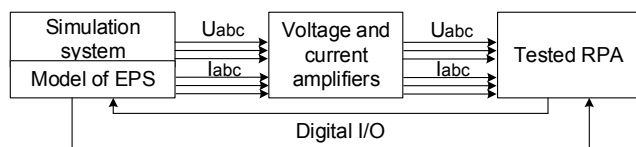


Fig.1. Bloch-diagram of HIL simulation

In Fig. 2 the examples of such testing scheme, wherein the part of EPS and the protected object are modelled in the HRTSim, while the developed complex of pulse-modulation amplifiers (PMAMP), which includes the voltage and current amplifiers (VAMP and IAMP) to interconnect with the real tested RPA.

In this paper the results of the development of PMAMP, including three VAMP units and three IAMP, a power supply block (12 V/200 A), comparison of the developed VAMP and IAMP with existing analogues by the main parameters of amplifiers, as well as evaluation of the regulation characteristic of the VAMP and IAMP, the value of gains depending on the frequency of input signals and the phase accuracy of the output signal is presented.

Main Principles Of Deveplemoed Of The PMAMP

The VAMP units are based on a class-D amplifiers, in which a high accuracy of the output voltage is achieved by

the use of serially connected autonomous voltage inverters. Each of these inverters has an independent power source and generates an output voltage in a certain zone from the total range of output signal variation, which represents a multi-zone pulse modulation [9, 10].

The functional scheme of the VAMP (Fig. 3) includes four identical cells - a bridge voltage inverters, the control system of which is provided by a programmable logic integrated circuit (or field-programmable gate array (FPGA) [11]). In this scheme, negative analog-digital feedback includes a summing amplifier, a correction unit and the FPGA.

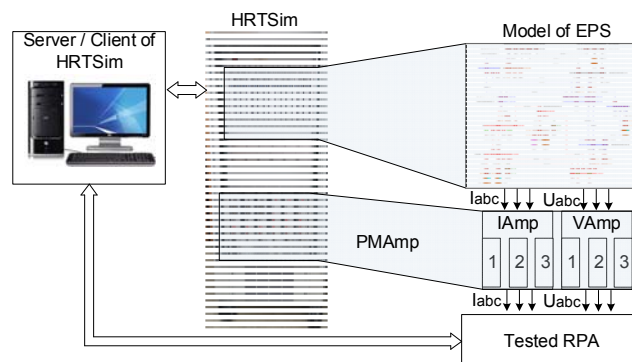


Fig.2. Bloch-diagram of HIL simulation

The application of this negative-feedback with the high modulation frequency $f = 100\text{kHz}$ and the small calculated frequency of the output LC filter, provides the minimum phase deviation in a given frequency range of the output signal.

According to the principle operation of bridge voltage inverters, when the any diagonal transistor switches are closed, a positive or negative half-wave of the output voltage is formed; accordingly, when the state of all transistor switches is locked, a zero voltage level is formed. Thus, it is possible to add or exclude the voltage source in the circuit, thereby carrying out multi-zone pulse modulation within eight zones [9, 10].

The IAMP units are similarly based on a class-D amplifiers, however, the outputs of all four bridge voltage inverters are connected in parallel through output chokes (L), which will also allow generating the output current of any form in a given frequency range. This scheme (Fig. 3) allows solving the task of converting the input signal (U_{in}) into the proportional output current (I_{out}).

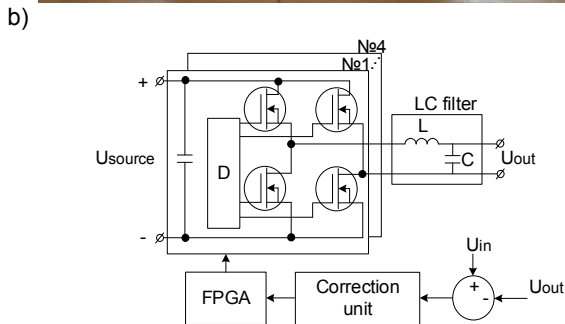


Fig. 3. The external appearance (a) and functional scheme (b) of the VAmP, where D - driver

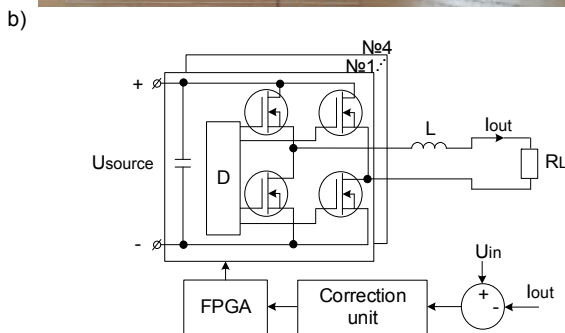


Fig. 4. The external appearance (a) and functional scheme (b) of the IAmp

The analysis of modern existing amplifiers used in HIL simulation

In Table 1 the main parameters of widely amplifiers, used in HIL simulation, and the developed VAmP and IAmp are presented.

According to the analysis and comparison, it can be seen that:

- the range of three-phase output voltage (U_{max}) and current (I_{max}) of VAmP and IAmp is not inferior (and even exceeds) the considered amplifiers;
- the frequency range (f_{max}) of output voltage and current, equal to 1000 Hz , covers a significant weight of

frequency spectrum processes in EPS, including switching overvoltage;

- the value of absolute error of phase shift angle of a sinusoidal signal (K_{nPh}) does not exceed the same coefficient of considered amplifiers;
- the value of voltage and current accuracy (K_{nU} and K_{nI}) of PMAmP exceed the analogous parameters of the considered amplifiers, but in general do not exceed 5%, which can be considered acceptable for an experimental sample.

To demonstrate the adequate operation of the PMAmP, the corresponding tests of VAmP and IAmp were carried out and the results are presented below.

To demonstrate the adequate operation of the PMAmP, the corresponding tests of VAmP and IAmp were carried out and the results are presented below.

Table 1. Characteristics of amplifiers, used in HIL simulation

Model	Parameters						
	I_{max} , A	K_{nI} , A	U_{max} , V	K_{nU} , V	f_{max} , kHz	K_{nPh} , %	
Retom-61 [12]	3ph	72	± 0.6	135	± 0.5	1	± 0.3
	1ph	200	± 4.8	405	± 4.9	2,1	
Retom -71 [13, 14]	3ph	40	± 0.6	135	± 0.5	1	± 0.1
CMS 356 [15]	3ph	64	± 0.05	300	± 0.09	1	± 0.05
	1ph	128	/	600	/	1	/
PAC2000C [16]	1ph	200	0.2	-	-	5	0.2
PAC60Cip [16]	3ph	60	0.06	-	-	5	0.2
PAV250Bi [16]	6ph	-	-	250	± 0.25	3	0.2
PMAmP:							
IAmp	3ph	100	± 2	-	-	1	0.1
VAmP	3ph	-	-	300	± 0.6	1	0.1

Tests of VAmP and IAmp units of PMAmP

The test program of the VAmP and IAmp units of PMAmP includes checking of the regulation characteristic, the value of gains depending on the frequency of input signals, the determination of the phase accuracy of the output signal.

The VAmP testing scheme (Fig. 5) includes a voltage source, voltmeters (V) and a load: resistor ($R = 900\text{ Ohm}$) and choke ($R = 380\text{ Ohm}, L = 2.3\text{ H}$).

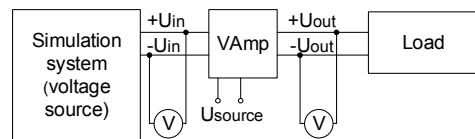


Fig. 5. The VAmP testing scheme

After supplying the power to the VAmP, the input voltage (U_{in}) in the range from 0 to 10 V (amplitude value) and with a frequency from 0 to 1000 Hz is set. The value of gain (K_{nU_exp}) is determined by the value measured effective value of the output voltage (U_{outRMS}) and its deviation from the nominal value ($K_{nU_nom} = 30$) is estimated. The results of the experiments and calculations are presented in Table 2.

$$\Delta = \frac{|K_{nU_nom} - K_{nU_exp}|}{K_{nU_nom}} \cdot 100\% - \text{deviation of } K_{nU}, \%$$

Based on the obtained results, it can be noted that Δ does not exceed 5%, and the transfer characteristic of the

Vamp has a linear relationship (Fig. 6), which generally confirms the adequacy of the developed Vamp unit.

Table 2. The results of the experiments and calculations of Vamp parameters

U_{inRMS}, V	R load					
	$f = 10 Hz$			$f = 1000 Hz$		
	U_{outRMS}, V	K_{nU_exp}	$\Delta, \%$	U_{outRMS}, V	K_{nU_exp}	$\Delta, \%$
0.71	21.40	30.27	0.90	21.90	30.67	2.24
1.41	42.40	29.99	0.05	43.40	30.69	2.31
2.12	63.50	29.94	0.20	64.60	30.46	1.52
2.83	84.70	29.95	0.17	85.80	30.34	1.13
3.54	105.80	29.92	0.27	109.10	30.64	2.12
4.24	127.20	29.98	0.07	130.67	30.80	2.66
4.95	148.50	30.00	0.01	151.70	30.65	2.15
5.66	169.60	29.98	0.06	174.00	30.76	2.53
6.36	190.70	29.97	0.12	196.40	30.86	2.87
7.07	211.70	29.94	0.20	218.50	30.90	3.00

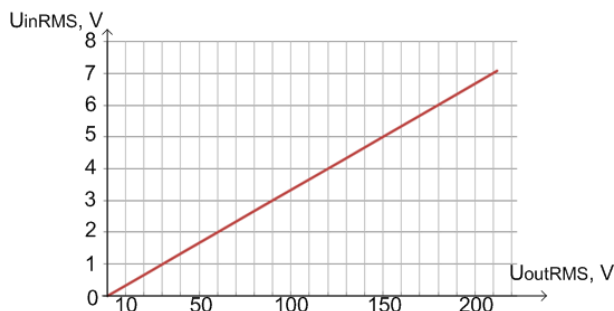


Fig. 6. The transfer characteristic of the Vamp for $f = 50 Hz$ and RL load

To confirm the adequacy of the frequency characteristics of the Vamp, the changes of the Δ depending on the frequency of the input signal are presented in the Table 3, in case when multifunctional measuring transmitters (MIP-02) [17] is used as a load.

Table 3. The value of Δ depending on the frequency of the input signal

f, Hz	$U_{in} = 5 V$			$U_{in} = 10 V$		
	U_{outRMS}, V	K_{nU_exp}	$\Delta, \%$	U_{outRMS}, V	K_{nU_exp}	$\Delta, \%$
10	21.40	30.17	0.58	211.70	29.94	0.19
50	21.43	30.03	0.09	215.20	30.44	1.46
100	21.50	30.15	0.51	216.30	30.59	1.98
150	21.56	30.21	0.71	217.10	30.71	2.36
400	21.02	29.46	1.81	217.50	30.76	2.55
800	21.35	29.90	0.33	217.80	30.81	2.69
1000	21.90	30.67	2.24	218.50	30.90	3.00

According to the amplitude-frequency characteristic of Vamp (Fig. 7), the value of the K_{nU} does not exceed 5% in the range up to 1000 Hz.

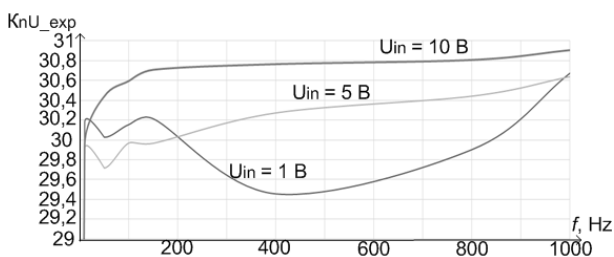


Fig. 7. Amplitude-frequency characteristic of Vamp

To estimate the phase shift angle of a sinusoidal signal (K_{nPh}), a phase meter (F2-34) and voltage dividers (R_{1-4}) were added to the Vamp testing scheme (Fig. 8). The value of R_{1-4} are selected in such a way to get the same level of 1.5 V at the inputs of the phase meter.

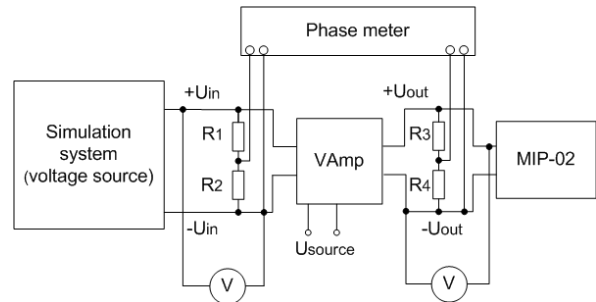


Fig. 8. The Vamp testing scheme for estimation the phase shift angle of a sinusoidal signal, where $R_1 = 10 kOhm$, $R_2 = 10 kOhm$, $R_3 = 30 kOhm$, $R_4 = 510 Ohm$

The results of measuring the phase deviation of the output voltage depending on the frequency of the input signal are presented in Table 4 and show an acceptable value of the phase shift (no more than 0.1°) and the correctness of the operation of the Vamp unit in the specified frequency range.

Table 4. Phase deviation of the output voltage of Vamp depending on the frequency of the input signal

f, Hz	U_{inRMS}, V	U_{outRMS}, V	The value of phase shift	
			$t, \mu s$	phase, $^\circ$
10	3.54	105.80	0.09–0.40	0.0016–0.0072
50	3.56	105.70	0.01–0.25	0.0002–0.0045
100	3.56	106.60	0.03–0.16	0.0005–0.0029
300	3.56	106.65	0.23–0.27	0.0041–0.0049
500	3.56	107.77	0.97–1.01	0.0175–0.0182
800	3.56	110.29	2.86–2.87	0.0515–0.0517
1000	3.56	112.10	3.35–3.51	0.0603–0.0632

The Iamp testing scheme (Fig. 9) includes a current source and Hall sensor (LEM LT 300-S/SP2). In this scheme the outputs of Iamp is shorted by a wire PV3 16 mm with a length $l = 0,35 m$.

After supplying the power to the Vamp, the input voltage (U_{in}) in the range from 0 to 10 V (amplitude value) and with a frequency from 0 to 1000 Hz is set. The value of gain (K_{nI_exp}) is determined by the value measured effective value of the output current (I_{outRMS}) and its deviation from the nominal value ($K_{nI_nom} = 10$) is estimated. The results of the experiments and calculations are presented in Table 5.

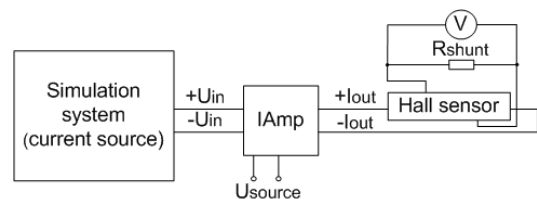


Fig. 9. The Iamp testing scheme, where R_{shunt} – value of shunt resistance (type CF-0.25)

Table 5. The results of the experiments and calculations of IAmp parameters

U_{inRMS}, V	$f = 10 Hz$			$f = 1000 Hz$		
	I_{outRMS}, A	K_{nl_exp}	$\Delta, \%$	I_{outRMS}, A	K_{nl_exp}	$\Delta, \%$
0.71	6.92	9.74	2.57	6.97	9.80	1.99
1.41	13.94	9.83	1.69	14.02	9.87	1.27
2.12	20.97	9.86	1.43	21.10	9.90	1.01
2.83	27.92	9.87	1.31	28.22	9.91	0.89
3.54	34.96	9.88	1.19	34.98	9.92	0.80
4.24	41.94	9.89	1.13	42.13	9.93	0.72
4.95	49.44	9.89	1.12	49.72	9.93	0.69
5.66	55.94	9.89	1.07	56.27	9.93	0.66
6.36	63.18	9.90	1.04	63.18	9.94	0.62
7.07	70.12	9.90	1.03	70.59	9.94	0.61

$$\Delta = \frac{|K_{nl_nom} - K_{nl_exp}|}{K_{nl_nom}} \cdot 100\% - \text{deviation of } K_{nl}, \%$$

Based on the obtained results, it can be noted that Δ does not exceed 5%, and the transfer characteristic of the IAmp has a linear relationship (Fig. 10), which generally confirms the adequacy of the developed IAmp unit.

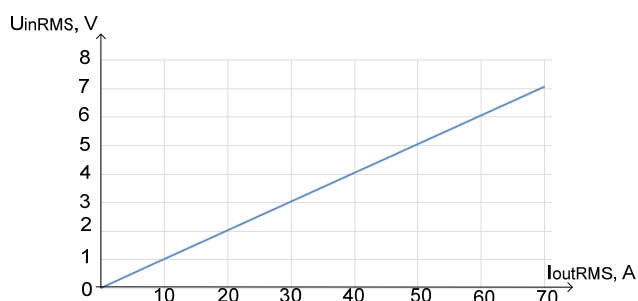


Fig. 10. The transfer characteristic of the IAmp for $f = 50 Hz$

To confirm the adequacy of the frequency characteristics of the IAmp, the changes of the Δ depending on the frequency of the input signal are presented in the Table 6, in case when Sepam-40 relay protection system is used as a load.

Table 6. The value of Δ depending on the frequency of the input signal

f, Hz	$U_{in} = 5 V$			$U_{in} = 10 V$		
	I_{outRMS}, A	K_{nl_exp}	$\Delta, \%$	I_{outRMS}, A	K_{nl_exp}	$\Delta, \%$
10	34.87	9.85	1.45	69.92	9.87	1.26
50	35.05	9.85	1.46	69.92	9.86	1.36
100	34.96	9.83	1.72	69.92	9.86	1.41
150	35.00	9.84	1.65	69.92	9.86	1.43
400	34.91	9.81	1.93	69.64	9.81	1.87
800	34.68	9.74	2.61	73.02	10.34	3.43
1000	35.21	9.89	1.12	74.17	10.44	4.40

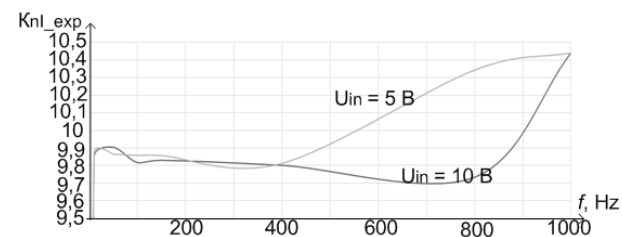


Fig. 11. Amplitude-frequency characteristic of Vamp

According to the amplitude-frequency characteristic of VAmp (Fig. 11), the value of the K_{nl} does not exceed 5% in the range up to 1000 Hz.

To estimate the phase shift angle of a sinusoidal signal (K_{nPh}), a phase meter (F2-34) and voltage dividers (R_{1-2}) were added to the IAmp testing scheme (Fig. 12). The value of R_{1-2} are selected in such a way to get the same level of 1V at the inputs of the phase meter.

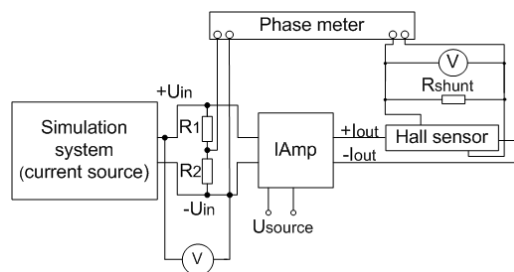


Fig. 12. The IAmp testing scheme for estimation the phase shift angle of a sinusoidal signal, where $R_1 = 39 kOhm$, $R_2 = 6.8 kOhm$

The results of measuring the phase deviation of the output current depending on the frequency of the input signal are presented in Table 7 and show an acceptable value of the phase shift (no more than 0.1°) and the correctness of the operation of the IAmp unit in the specified frequency range.

Table 7. Phase deviation of the output current of IAmp depending on the frequency of the input signal

f, Hz	U_{inRMS}, V	I_{outRMS}, A	The value of phase shift	
			$t, \mu s$	phase, $^\circ$
10	7.07	69.91652	0.05–0.035	0.00063–0.0009
50	7.07	69.91652	0.01–0.48	0.00018–0.00864
100	7.07	69.91652	0.02–0.04	0.00036–0.00072
300	7.07	69.91652	1.06–1.07	0.01908–0.01926
500	7.07	69.63981	1.57–1.59	0.02826–0.02862
800	7.07	73.42157	1.83–1.85	0.03294–0.0333
1000	7.07	75.5221	2.01–2.25	0.03618–0.0405

The results of the tests of the developed VAmp and IAmp units of the PMamp show the adequacy of the output voltage and current: the deviation of the gain of the VAmp and IAmp does not exceed 5% in the range up to 1000 Hz, and the phase deviation of the output voltage and current does not exceed 0.1° .

It should be note, that the output current of the IAmp can be increased up to 200 A (in amplitude), but it requires the increasing of the supply voltage and the overall power of the converters will increase up to 4.5 kW.

Conclusion

The results of the development and testing of the complex of pulse-modulation amplifiers (PMamp), which includes the voltage and current amplifiers (VAmp and IAmp), are presented.

The comparison of the developed VAmp and IAmp with existing analogues by the main parameters of amplifiers shows that VAmp and IAmp units of PMamp can be used in HIL simulation of the real RPA, in particular the range of three-phase output voltage and current of VAmp and IAmp is not inferior (and even exceeds) the considered amplifiers.

At the same time, the obtained test results show the adequate operation of the amplifiers: the deviations of the

gains, the accuracy and phase accuracy of the output voltage and current were determined, which do not exceed 5% and 0.1⁰, respectively.

Acknowledgment

The work is performed with financial support of the Ministry of Science and Higher Education of the Russian Federation. Grant agreement RFMEFI57818X0272.

Authors: Associate professor of Division for Power and Electrical Engineering, Ruslan Ufa, Tomsk Polytechnic University, 30, Lenin Avenue, Tomsk, Russia, E-mail: hecn@tpu.ru; associate professor of Division for Power and Electrical Engineering, Mikhail Andreev, Tomsk Polytechnic University, 30, Lenin Avenue, Tomsk, Russia, E-mail: andreevmv@tpu.ru; student of Division for Power and Electrical Engineering, Rudnik Vladimir, Tomsk Polytechnic University, 30, Lenin Avenue, Tomsk, Russia, E-mail: fordlp006@mail.ru; associate professor of Division for Power and Electrical Engineering, Yudin Svyatoslav, Tomsk Polytechnic University, 30, Lenin Avenue, Tomsk, Russia, E-mail: yudinsm@tpu.ru; associate professor of Division for Power and Electrical Engineering, Kosmynina Nina, Tomsk Polytechnic University, 30, Lenin Avenue, Tomsk, Russia, E-mail: kosm_nm@tpu.ru.

REFERENCES

- [1] Avalos A., Zamora A., Escamilla O., Paternina M. R. A., Real-time Hardware-in-the-loop Implementation for Power Systems Protection. IEEE PES Transmission & Distribution Conference and Exhibition - Latin America (T&D-LA), 18-21 Sept. 2018, Lima, Peru, P. 1-5.
- [2] Cui Q., El-Arroudi Kh., Joós G., Real-time hardware-in-the-loop simulation for islanding detection schemes in hybrid distributed generation systems. *IET Generation, Transmission & Distribution*, 11 (2017), No. 12, pp. 3050-3056.
- [3] Penczek A., Stala R., Stawiarski L., Szarek M. Hardware-in-the-loop FPGA-based simulations of switch-mode converters for research and educational purposes. *Przegląd Elektrotechniczny*, 87 (2011), No. 11, pp. 194-200.
- [4] Xue Y., Kong D., Guan R., Li J., Taylor A., Zhang X-P., RTDS-based HIL testing platform for complex modern electricity transmission systems. *J. Eng.*, 2018 (2018), No. 15, pp. 1315-1320.
- [5] Nawrot R., Miński R., Wasiak I., The method of designing the energy storage control algorithm in a prosumer installation using Real-Time Simulator RTDS. *Przegląd Elektrotechniczny*, 94 (2018), No. 11, pp. 166-169.
- [6] Dufour Ch., Cense S., Jalili-Marandi V., Bélanger J., Review of state-of-the-art solver solutions for HIL simulation of power systems, power electronic and motor drives, EPE'13 ECCE Europe conference, 3-5 September 2013, Lille, France, P. 1-12.
- [7] Andreev M., Gusev A., Ruban N., Suvorov A., Ufa R., Askarov A., Bemš J., Králík T., Hybrid real-time simulator of large-scale power systems. *IEEE Transactions on Power Systems*, 34(2019), No. 2, pp. 1404-1415.
- [8] Andreev M., Borovikov Y., Gusev A., Sulaymanov A., Ruban N., Suvorov A., Ufa R., Bemš J., Králík T., Application of hybrid real-time power system simulator for research and setting a momentary and sustained fast turbine valving control. *IET Generation, Transmission and Distribution*, 12 (2018), No. 1, pp. 133-141.
- [9] Kobzev A., Pulse-multizone modulation. A theory and application is in the systems of transformation of parameters of electric energy. Novosibirsk: Nauka, 1979, 304 p.
- [10] Kobzev A., Lebedev Yu., Mikhalchenko G., Semenov V., Sidonsky I., Taraskin A., *Stabilizatory peremennogo napryazheniya s vysokochastotnym shirotno-impul'snym regulirovaniem* (AC Voltage Stabilizers with High-Frequency Broad-Band Control). Moscow: Energoatomizdat, 1986, 152 p.
- [11] Przybył A., Szczypa J., Method of evolutionary designing of FPGA-based controllers. *Przegląd Elektrotechniczny*, 92 (2016), No. 7, pp. 174-179.
- [12] BRGA.441323.017 RÉ RETOM-61, Programmable Technical Measuring System. Operations Manual [in Russian] [Online]. Available: <http://dynamics.com.ru/userfiles/file/support/retom-61.pdf> [Accessed: 11.06.2019].
- [13] BRGA.441323.035 RÉ RETOM-71, Programmable Technical Measuring System. Operations Manual [in Russian] [Online]. Available: <http://dynamics.com.ru/userfiles/file/support/retom-71.pdf> [Accessed: 11.06.2019].
- [14] Zaytcev B., Shalimov A., Application of the test system RETOM-71 for multi-functional protective relays and systems of relay protection and automation. *Advancement of Relay Protection, Automation and Control in Electric Power Engineering*, 25 (2016), No. 4, pp. 45-48.
- [15] CMS 356 Voltage and current amplifier, Technical-Data [Online]. Available: <https://www.omicronenergy.com/en/products/cms-356/> [Accessed: 11.06.2019].
- [16] Power Amplifier for Real Time Digital Simulation, Technical-Data [Online]. Available: http://www.relaytest.com/userfiles/file/Catalogs/RTDS_Amplifier_Brochure.pdf [Accessed: 11.06.2019].
- [17] Multifunctional measuring transmitters, Technical-Data [in Russian] [Online]. Available: <http://www.rtsoft.ru/upload/pdfcat/MIP-02.pdf> [Accessed: 11.06.2019].